Journal of Thermal Analysis and Calorimetry, Vol. 64 (2001) 341–350

A NOVEL SINGLE-PAN SCANNING CALORIMETER Measurement of thermophysical properties of metallic alloys

H. B. Dong and J. D. Hunt

Department of Materials, University of Oxford, Parks Road, Oxford OX1 3PH, United Kingdom

Abstract

In this paper problems associated with a conventional heat-flux DSC are discussed. A single pan calorimeter has been designed and built which eliminates many of the errors that occur in a conventional DSC. It was found that: enthalpy changes and heat capacity were repeatable to better than 1%; the apparent latent heat and heat capacity did not depend on specimen size or significantly on rate of heating as often occurs in a two-pan heat-flux DSC; during the melting of pure Al, more than 80% of the latent heat was evolved over a temperature of 0.04 K; in alloys, separate heat capacity peaks for different reaction less than 1 K apart were resolved.

Keywords: calorimetry, enthalpy change, heat capacity, heat-flux DSC, metallic alloy, temperature measurement

Introduction

Differential scanning calorimetry (DSC) consists of a reference pan and a sample pan contained in a constant temperature enclosure (Fig. 1a). Typically in the heat-flux method the enclosure temperature is increased or decreased at a constant rate.

In Fig. 2a, the enclosure temperature T_F, reference pan temperature T_{RP} and sample pan temperature T_{SP} are plotted schematically *vs.* time. As the enclosure temperature rises at a constant rate, the sample pan and reference pan temperature rise at the same rate; when the pure metal sample begins to melt, the sample temperature T_S remains constant until the sample is completely melted. When melted, T_S rises rapidly and again eventually reaches a steady state difference. The temperature differences $\Delta T_{FS}=T_F-T_{SP}$ and $\Delta T_{FR}=T_F-T_{RP}$ are plotted *vs.* time t, in Fig. 2b. Assuming heat-fluxes are proportional to the temperature difference between the sample and the surroundings means that the product of the temperature difference and time is proportional to the enthalpy change. The hatched areas in Fig. 2b are proportional to the enthalpy changes from times t_1 to t_2 in the sample and reference.

It is often assumed that the temperature difference, $\Delta T_{RS}=T_{RP}-T_{SP}$ is proportional to the difference in heat capacity between the sample and reference. This is true when

1418–2874/2001/ $ 5.00

Akadémiai Kiadó, Budapest
Kluwer Academic Publishers, Dordrecht

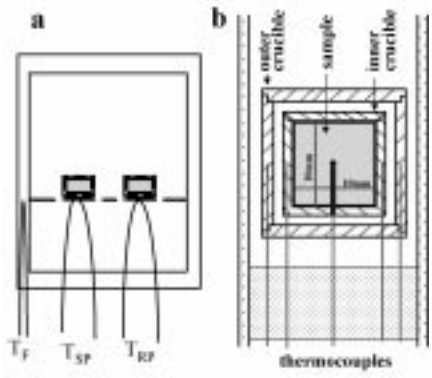

Fig. 1 Schematic diagram of a conventional heat-flux DSC (a); Schematic diagram of the calorimeter described in the present work (b)

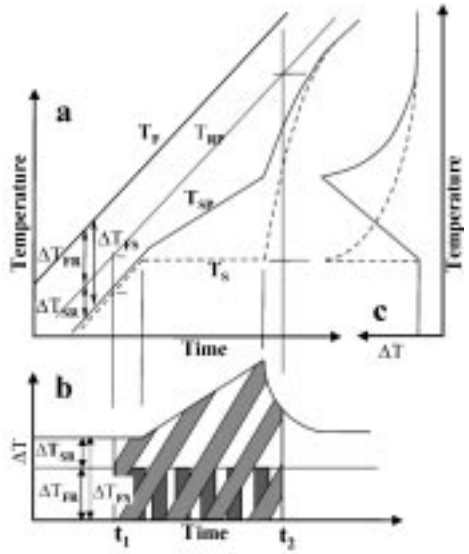

Fig. 2 A combined schematic plot of a – temperature *vs.* time; b – temperature difference *vs.* time; c – temperature difference *vs.* temperature for a heat-flux DSC

the sample and reference temperature change at the same rate, but is not true when the changes are different. This is apparent from Fig. 2c where the temperature differences are plotted *vs.* temperature. Immediately after melting ΔT_{RS} is large because the sample temperature is rising more rapidly than the reference. Neglect of this effect leads to smearing of the temperature over which latent heat is apparently evolved [1].

Another problem arises with a heat-flux DSC. When large heat-fluxes are present, the thermocouples do not measure the actual temperature of the sample or reference. This is because the thermal resistance between the sample (or reference) and its thermocouple is significant when compared with the thermal resis-

tance between the thermocouple and the surroundings. To a first approximation the two temperature differences $T_F - T_{SP}$ and $T_{SP} - T_S$ are expected to be proportional to one another. This results in the sample thermocouple temperature T_{SP}, plot *vs.* time shown by the solid line in Fig. 2a and the plot of apparent temperature difference *vs.* temperature as the solid line in Fig. 2c. The important feature is that even though the sample melts at one temperature heat appears to be smeared or absorbed over a range of temperatures.

These two effects explain why it is generally recognised that small samples must be used in a two-pan calorimeter to reduce smearing when a significant amount of latent heat is evolved. Unfortunately small samples lead to greatly reduced heat-fluxes and loss of accuracy.

It is difficult to see the reason for using a reference pan. The difference in temperature between the sample and the enclosure contains similar information to that of the temperature difference between sample and reference (Fig. 2b). In addition the absence of a reference pan means the heat flow within the enclosure is geometrically simple and analysis can be easily used to eliminate smearing even for large samples. These considerations led to the development of a single-pan calorimeter.

The new single-pan scanning calorimeter

The essential feature of the calorimeter is that the sample is in a uniform temperature enclosure and that it has the largest possible thermal resistance between the sample and its surroundings. A schematic diagram of the apparatus is shown in Fig. 1b. To ensure a uniform temperature enclosure, the outer crucible was thermally isolated from the furnace, was thick walled and made of a material with a high conductivity. The inner crucible was thermally isolated from the outer crucible to ensure the maximum temperature difference between the two crucibles. In principle there is no disadvantage in using large samples provided significant temperature differences do not arise in the sample. Thermocouples 0.5 mm OD were placed in the walls of the inner and outer crucibles. An additional thermocouple was placed in the centre of the sample.

The calorimeter could be operated in the normal DSC manner by changing the outer crucible temperature at a programmed rate. Because the specimens were much larger than a conventional heat-flux DSC, the calorimeter could be operated in a constant heat-flux mode as was proposed by Smith 1940 [3]. In this mode the temperature difference between the inner and outer crucibles is kept constant. This means the temperature rises less rapidly when latent heat is absorbed. The calorimeter could also be operated in a temperature modulated mode.

Since the specimen is large the calorimeter is ideally suited for slow heating or cooling rates. Significant results could be obtained with heating rates as low as 0.1 K min^{-1} even so heating and cooling rates of 30 K min^{-1} were achieved.

Enthalpy calculation

Because of the simplicity of the single-pan calorimeter, equations are easily derived to relate temperature changes to enthalpy changes and to eliminate smearing. As in a conventional DSC a run was carried out with an empty pan, the (empty pan+calibrant), and the (empty pan+sample). The temperature differences were first corrected with a zero line adjustment. These were measured during an isothermal anneal [1] before, during and after a run.

As the calorimeter is heated in the time interval dt the temperature of the empty inner crucible rises dT_E, the (calibrant+empty) rises dT_C and the (sample+empty) rises by dT_S. The corresponding temperature differences between the inner and outer crucible for the three cases are ΔT_{DE}, ΔT_{DC} and ΔT_{DS}. Let C_C be the change in heat content per degree (i.e. heat capacity times mass) of the calibrant; this must be known as a function of temperature. Similarly C_E and C_S are those of the empty crucible and sample. It should be noted that C_S contains any latent heat and is thus an effective heat capacity. The heat transfer coefficient between the inner and outer crucible is α and will be a function of temperature.

For the empty crucible $\alpha\Delta T_{DE}\mathrm{d}t=C_E\mathrm{d}T_E$

For the calibrant+empty $\alpha\Delta T_{DC}\mathrm{d}t=(C_C+C_E)\mathrm{d}T_C$

For the sample+empty $\alpha\Delta T_{DS}\mathrm{d}t=(C_S+C_E)\mathrm{d}T_S$

Eliminating α and C_E gives a general expression for the rise in enthalpy of the sample dH_S.

$$C_C\left(\frac{\Delta T_{DS}-\frac{\Delta T_{DE}}{\mathrm{d}T_E}\mathrm{d}T_S}{\frac{\Delta T_{DC}}{\mathrm{d}T_C}-\frac{\Delta T_{DE}}{\mathrm{d}T_E}}\right)=C_S\mathrm{d}T_S=\mathrm{d}H_S \qquad (1)$$

The equation is valid as $\mathrm{d}T_S\rightarrow 0$ and can thus handle the latent heat of a pure material. The ratios $\Delta T_{DE}/\mathrm{d}T_E$ and $\Delta T_{DC}/\mathrm{d}T_C$ are evaluated from the empty and calibrant+empty run at the relevant temperature using the same time interval. The meaning of these terms is best visualised by noting that the first is the inverse of $(\mathrm{d}T_E/\mathrm{d}t)(1/\Delta T_{DE})$ which is the rate of rise of the empty pan divided by the difference in temperature between the inner and outer crucible. The general equation is valid for any mode of operation and that includes constant rate of temperature rise or constant heat-flux. It should be emphasised that the equation and use of a central thermocouple automatically handles the de-smearing process.

Results and discussion

In the present work Cu was used as the calibrant using data from [4]. A number of materials have been investigated. In this paper, the results for pure Al, a binary Al–(0.2 mass%)Fe and an Al alloy (LM25) will be reported.

Pure Al

Melting range of Al

Figure 3 shows the sample temperature plotted *vs.* time for pure Al. In these experiments the temperature difference between the inner and outer crucible was set to ±6 K. The inner crucible was alumina and the outer crucible boron nitride; this gave a heating rate in the absence of latent heat evolution of about 3.4 K min^{-1}. The temperature variation during melting and solidification was very small; 82% of the latent heat was evolved over 0.04 K and 50% of the latent heat evolved over 0.01 K.

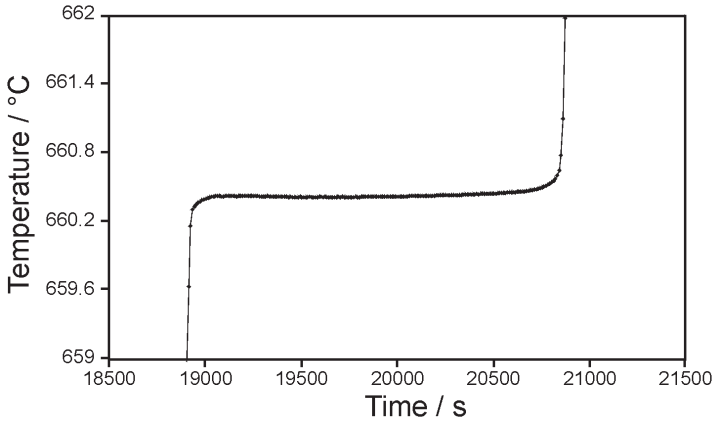

Fig. 3 Measured temperature range *vs.* time for pure Al with single-pan calorimeter at constant temperature difference 6 K

Enthalpy change and heat capacity measurement

Enthalpy changes were calculated by using the experimental results to integrate Eq. (1). Figure 4a shows the enthalpy for pure Al plotted as a function of temperature. The melting and freezing lines almost coincide. Figure 4b shows the heat capacity obtained using the slope of Fig. 5a for the melting line. Note the small difference in heat capacity before and after melting. Another important feature is the narrowness of the latent heat peak. It is not possible to get such a narrow peak with a conventional heat-flux DSC for the reasons discussed in the introduction. Very good reproducibility was obtained; the average values and standard deviation for seven runs for heat capacity and latent heat are compared with [4] in Table 1 and show runs carried out with

different heat-fluxes. Much less than 1% variation was obtained between samples and runs using the same sample.

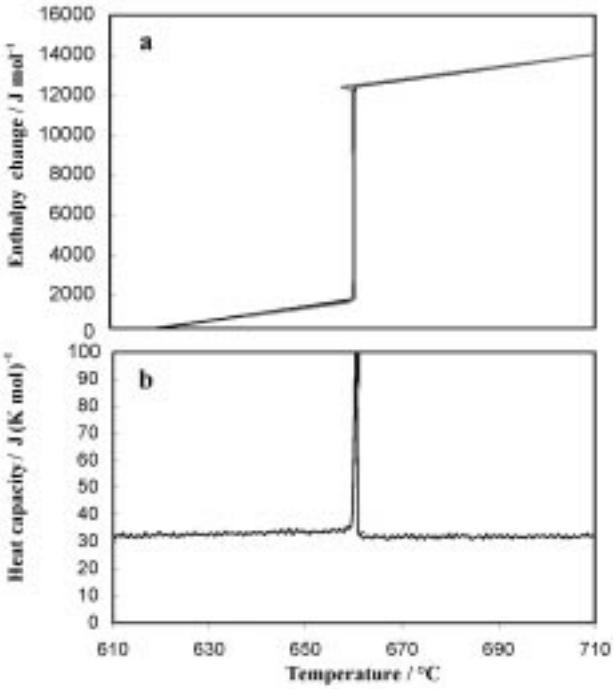

Fig. 4 Plots using pure Al for a – enthalpy change *vs.* temperature during melting and freezing; b – effective heat capacity *vs.* temperature for melting. Constant temperature difference 6 K

Table 1 Measured results on pure Al of the single-pan calorimeter

	C_p at 600°C/	C_p at 650°C/	C_p at 670°C/	L (heating)/	L (cooling)/
	J mol^{-1} K^{-1}			J mol^{-1}	
Results for seven runs using pure Al					
Averaged	31.5643	33.2529	31.40	10932	10910
Standard deviation	±0.1349	±0.1874	±0.1460	±29.31	±35.36
Hultgren *et al*. 1973	31.52	33.14	31.72	10784±125	
Results for pure Al using different heating/cooling rates					
1.5 K min^{-1}	31.45	33.20	31.40	11028	10820
3.4 K min^{-1}	31.56	33.25	31.40	10932	10910
4.5 K min^{-1}	31.50	33.40	31.50	10820	10630

Binary (Al–0.2 mass% Fe)

Figure 5a and b show the enthalpy change and heat capacity of Al–0.2 mass% Fe plotted as a function of temperature using a constant heat-flux. The average and standard deviation of six runs results, for the non-equilibrium solidus, non-equilibrium liquidus, heat capacity and latent heat are given in Table 2. Again very good reproducibility was obtained.

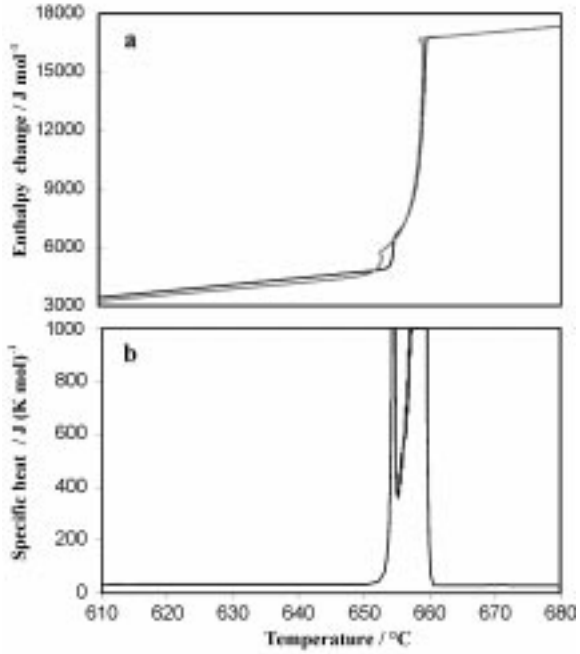

Fig. 5 Plots using Al–0.2 mass% Fe for a – enthalpy change *vs.* temperature during melting (dark line) and freezing (grey line); b – effective heat capacity *vs.* temperature for melting. Constant temperature difference 6 K

Alloy LM25 (Al – 7.3 mass% Si, 0.37 mass% Fe, 0.16 mass% Mn, 0.46 mass% Mg, 0.07 mass% Cu)

Figure 6a–c shows the enthalpy change and effective heat capacity for LM25 measured using a constant heat-flux. The enthalpy line is different for melting and freezing and is consistent with a departure from equilibrium as freezing takes place. The effective heat capacity for melting, Fig. 6b, and for freezing, Fig. 6c, shows a number of transitions. On freezing Al dendrites were formed at about 620°C and continued to be deposited until a eutectic (Al+Si) came out at about 570°C; finally a ternary eutectic (Al+Si+β) was deposited at about 550°C. On heating the lowest temperature peak splits into two separated by about 2 K. The additional peak was found to be the result of a solid-state deposit of Mg_2Si. Reactions of the ternary and solid-state deposit were not detected by [5] in a conventional heat-flux DSC. The results from elec-

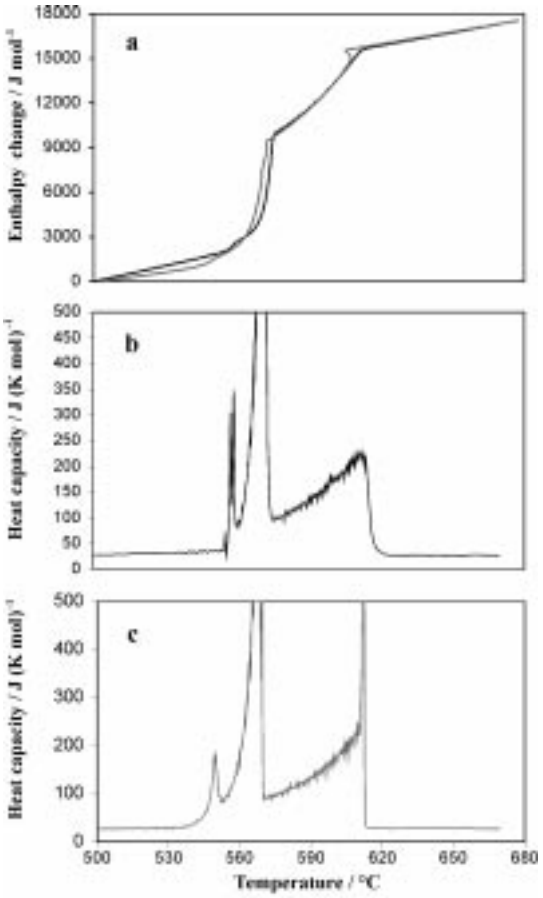

Fig. 6 Plots using LM25 for a – enthalpy change *vs.* temperature during melting (dark line) and freezing (grey line); b – effective heat capacity *vs.* temperature for melting; c – effective heat capacity *vs.* temperature for freezing. Constant temperature difference 6 K

tron microprobe analysis and XRD confirmed the existence of the β and Mg_2Si phases. Six runs were carried out to investigate reproducibility; the results, average and standard deviation, for the solidus, liquidus, heat capacity and latent heat are given in Table 2.

Conclusions

It is concluded that the present single-pan calorimeter has significant advantages over a conventional heat-flux DSC.

1. The analysis and set-up automatically removes the need for de-smearing.
2. High resolution is obtained for the onset of phase transformations.

Table 2 Results for six runs using Al–0.2 mass% Fe and LM25

	Non-equilibrium solidus/°C		Non-equilibrium liquidus/°C		C_p /	C_p/	Enthalpy change/J mol^{-1}	
	heating	cooling	heating	cooling	J mol^{-1} K^{-1}		heating	cooling
		Al–0.2 mass% Fe			(at 640°C)	(at 670°C)	(from 652 to 659°C)	
Averaged	654.29	652.49	658.56	658.49	33.78	31.74	11152	11178
Standard deviation	±0.18	±0.21	±0.10	±0.12	±0.22	±0.06	±32.0	±41
		LM25			(at 530°C)	(at 630°C)	(from 652 to 659°C)	
Averaged	555.60	547.81	618.26	613.03	37.54	31.86	17551	17480
Standard deviation	±0.43	±0.63	±0.10	±0.12	±0.28	±0.074	±57.97	±56.39

3. Accurate heat-fluxes can be measured because the heat flow path is well defined and the flux thermocouples measure temperature differences over the largest possible thermal resistance; reproducibility is better than 1%.

4. A constant heat-flux mode can be used thus minimising errors due to an increasing heat-flux.

References

1 G. Höhne, W. Hemminger and H.-J. Flammershein, Differential Scanning Calorimetry, Berlin, Springer 1996.
2 M. J. Richardson, In: Compendium of Thermophysical Property Measurement Methods, New York, Plenum Press 1992, p. 519.
3 C. S. Smith, Trans. Amer. Inst. Met. Eng., 137 (1940) 236.
4 R. Hultgren, P. D. Desai and D. T. Hawkins, Selected Values of the Thermodynamic Properties of Elements. ASM, Ohio 1973.
5 P. N. Quested, K. C. Mills, R. F. Brookes, A. P. Day, R. Taylor and H. Szelagowski, Proc. Int. Conf. on Solidification Processing, Sheffield University Press, July 1997, p. 143.